VOLTAMMETRIC STUDY OF 2-GUANIDINOBENZIMIDAZOLE: ELECTRODE MECHANISM AND DETERMINATION AT MERCURY ELECTRODE

Sławomira Skrzypek[a1,*], Valentin Mirčeski[b], Sylwia Smarzewska[a2], Dariusz Guziejewski[a3] and Witold Ciesielski[a4]

[a] *Department of Instrumental Analysis, University of Lodz, Pomorska 163, 90-236 Lodz, Poland; e-mail: [1] skrzypek@uni.lodz.pl, [2] sylwiasmarzewska@gmail.com, [3] dguziejewski@uni.lodz.pl, [4] ciesielski@uni.lodz.pl*

[b] *Institute of Chemistry, Faculty of Natural Sciences and Mathematics, "Ss Cyril and Methodius" University, P.O. Box 162, 1000 Skopje, Republic of Macedonia; e-mail: valentin@iunona.pmf.ukim.edu.mk*

Received June 17, 2011
Accepted July 27, 2011
Published online January 10, 2012

Although 2-guanidinobenzimidazole (GBI; CAS: 5418-95-1) is a compound of biological interest, generally there is a lack of electrochemical studies and the methods of its determination. The GBI behavior at a mercury electrode was analyzed under conditions of linear sweep voltammetry (LSV), differential pulse voltammetry (DPV), square-wave voltammetry (SWV) and square-wave stripping voltammetry (SWSV). Although GBI is electrochemically inactive at mercury electrode it adsorbs at the mercury surface and catalyzes effectively the hydrogen evolution reaction. Theoretical analysis of two possible pathways, according to which the GBI electrode mechanism can be explained, is performed. Simple analysis of peak current and potential with respect to available time window, i.e. change of frequency can be helpful in discerning the character of the recorded SW current. The established electrode mechanism is assumed to involve a preceding chemical reaction in which the adsorbed catalyst (GBI_{ads}) is protonated and the protonated form of the catalyst ($GBIH^{+}_{(ads)}$) is irreversibly reduced at potential about –1.18 V vs Ag|AgCl (citrate buffer pH 2.5). New methods of voltammetric determination of 2-guanidinobenzimidazole were developed. The detection and quantifications limits were found to be 1×10^{-7}, 1×10^{-6} mol l^{-1} (SWV); 8×10^{-8}, 9×10^{-7} mol l^{-1} (SWSV); 4×10^{-7}, 2×10^{-6} mol l^{-1} (DPV) and 6×10^{-7}, 3×10^{-6} mol l^{-1} (LSV), respectively.

Keywords: Electrochemistry; Trace analysis; Voltammetry; 2-Guanidinobenzimidazole; Nature of the electrode mechanism; Catalytic hydrogen evolution; Square-wave voltammetry.

Benzimidazoles are active compounds involved in a great variety of biological processes. Some of benzimidazole derivatives are the active components

Collect. Czech. Chem. Commun. 2011, Vol. 76, No. 12, pp. 1699–1715

doi:10.1135/cccc2011122

of fungicides and bactericides[1]. 2-Guanidinobenzimidazole (GBI; CAS: 5418-95-1) has important biological properties as it acts as a regulator of the transport of Na^+ and K^+ in the apical membrane of the skin, diminishes the gastric acid secretion, and serves as a hypoglycemiant and a hypotensor. Another important property of GBI is its activity on photosynthesis, acting as a mild uncoupler of photophosphorylation[2].

The compound is a polyfunctional planar molecule with a delocalized π electron system, where several conformers and tautomers are possible (Scheme 1). The structure and dynamical behavior of GBI have been studied in solution by ^1H, ^{13}C and ^{15}N NMR [3–5]. Also the protonation, coordination and methylation sites of GBI were investigated using NMR and X-ray diffraction[1]. Mercapto and thio derivatives of benzimidazole were studied with voltammetric[6,7], chromatographic[8,9] and spectrophotometric[10] methods; however, to the best of our knowledge, no study exists on the electrochemistry of GBI. Moreover, in spite of the obvious biochemical importance of GBI, yet there is a lack of chromatographic, as well as spectrophotometric methods of its quantification.

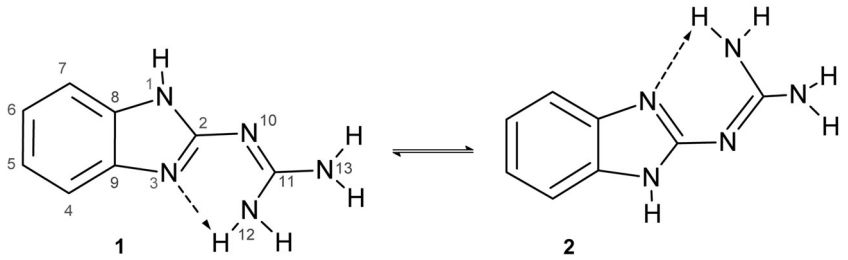

SCHEME 1
Conformers of 2-guanidinobenzimidazole[2]

In the present communication, the electrochemical behavior of GBI at the hanging mercury drop electrode (HMDE) is studied using voltammetric techniques, such as square-wave voltammetry (SWV), differential pulse (DPV) and linear sweep (LSV) voltammetry. The techniques are often successfully applied for analytical determinations of drugs[11,12] and pesticides[13–16].

The aim of the present work is to establish the main features of the electrode mechanism of GBI upon which a method for quantitative determination is developed. The voltammetric data are analyzed in the light of the theory referring to adsorptive accumulation of an electroactive compound followed by irreversible electrochemical reaction[17,18] and the hydrogen evo-

lution surface catalytic electrode mechanism[19] under conditions of SWV [20]. It is worth mentioning that hydrogen evolution surface catalytic mechanism has been encountered with various species having capability to adsorb on the HMDE surface and containing nitrogen atoms as a center of protonation, such as famotidine[19], metformine[20] and acyclovir[21]. Among various catalytic mechanisms, those based on the hydrogen evolution reaction are the most sensitive ones[22]. Different species exhibit catalytic effect toward hydrogen evolution reaction ranging from noble metal particles (e.g., Pd, Pt, Ir, Rh and Ru), transition metal complexes, and organic substances containing functional groups such as $–NH_2$, =NH, –SH and –COOH [23]. The present results also suggest that the compounds having the guanidine group –N=C(NH–)–NH– can also catalyze the hydrogen evolution reaction. Finally, we note that catalytic electrode reactions based on the hydrogen evolution has been proven to be of particular analytical utility for determination of compounds of pharmacological relevance[24].

EXPERIMENTAL

Instrumentation

The voltammetric experiments were performed with a micro-Autolab/GPES (General Purpose Electrochemical System, Version 4.8, Eco Chemie, Netherlands) computer-controlled electrochemical system. A controlled growth mercury drop electrode (Entech s.c., Cracow, Poland) was used. The mercury drop surface area was found to be 0.0102 cm^2. All potentials were referred versus Ag|AgCl (3 M KCl) reference electrode. The counter electrode was a platinum wire. Operating conditions were: scan rate 200 mV s^{-1} and step potential 3 mV for LSV; pulse amplitude 90 mV and step potential 3 mV for DPV; pulse amplitude 90 mV, frequency 100 Hz and step potential 15 mV for SWV. The following equipment was also used: pH-meter type CP-315M (Elmetron, Poland) and electronic scale type MC-1 (Sartorius, Germany).

Reagents and Solution

Fresh stock solution of 1×10^{-3} M GBI was prepared daily by dissolving 9.19 mg of the compound in 50 ml water. Citrate buffers (0.1 mol l^{-1}, pH 1.8–4), acetate buffer (0.2 mol l^{-1}, pH 3.6), citrate-phosphate buffer (0.2 mol l^{-1}, pH 2) and Britton–Robinson buffers (0.04 mol l^{-1}, pH 2–5) were used as supporting electrolyte. All chemicals were analytical grade (POCh SA Gliwice, Poland, Merck and Sigma–Aldrich). All solutions were prepared with triply distilled water.

Analysis Procedures

The general procedure used to obtain voltammograms was as follows: 10 ml of the supporting electrolyte was placed in the voltammetric cell and the solution was purged with argon for 10 min. When an initial blank was recorded, required volume of GBI aqueous solution was added by means of a micropipette. Then, the solution was deoxygenated for 30 s and

after formation of a new drop of Hg, an accumulation period of 50 s was applied without stirring at an accumulation potential of 0 V. Next a negative-going potential scan from 0 to –1.75 V was applied. To obtain a well-shaped voltammetric peak for measurements, the supporting electrolyte current was subtracted from the recorded GBI current. All experiments were performed at room temperature.

RESULTS AND DISCUSSION

Voltammetric Properties and Electrode Mechanism

Typical SW voltammetric response of GBI at the HMDE consists of a peak located at more negative potentials than –1.00 V, frequently emerging only as a shoulder at the residual current of the hydrogen reduction reaction (Fig. 1).

The forward and backward components of the SWV response indicate totally irreversible reduction mechanism (inset of Fig. 1). The overall voltammetric properties are typical for irreversible processes coupled with adsorption of the reactant, as the response is highly sensitive to the accumulation time. For GBI concentration of 5×10^{-7} mol l^{-1}, the peak current

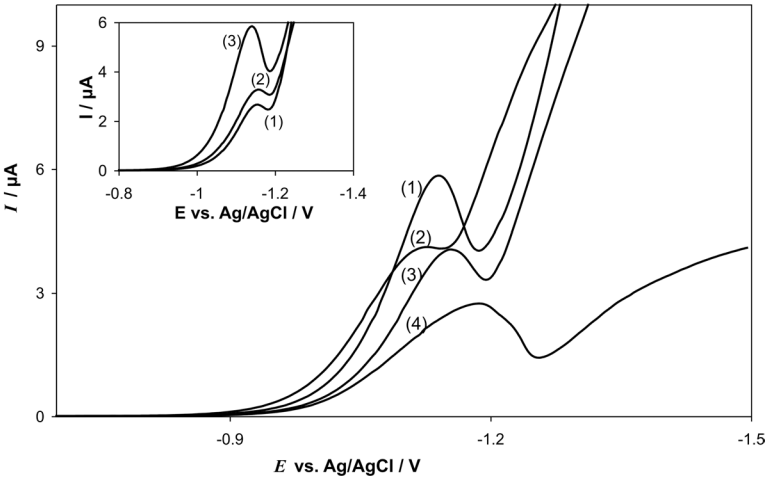

FIG. 1
Net SW voltammograms of 1×10^{-5} M GBI recorded in different buffer solutions at pH 2: citrate (1), citrate-phosphate (2), Britton–Robinson (3) and acetate (4) (pH 3.6) at accumulation time 5 s and initial potential 0 V. The parameters of the potential modulation were: frequency f = 25 Hz, amplitude E_{sw} = 20 mV and step potential ΔE = 5 mV. Inset: Typical SW voltammetric response of the 1×10^{-5} M GBI recorded in a citrate buffer at pH 2 depicting the net (1), anodic (2) and cathodic (3) components

increases linearly with the square root of the accumulation time up to 50 s accumulation. At prolonged accumulation, the peak current reaches a maximal value or commences decreasing. For instance, the SW net peak current was 9.46 and 3.57 μA for accumulation time of 30 and 180 s, respectively, implying that the electrode reaction is accompanied by complex surface phenomena. In addition, the overall voltammetric features are a function of the composition, concentration and pH of the buffer, as well as the parameters of the potential modulation, such as the SW frequency (*f*), the height of the SW pulses (i.e., amplitude (E_{sw})), and the step potential of the staircase potential ramp (ΔE)[25]. Figure 1 shows that the morphology of the response is strongly sensitive to the buffer type, the citrate buffer being the most suited medium taking into account the height (ΔI_p), half-peak width ($\Delta E_{p/2}$), and position (E_p) of the peak, providing well separation from the residual current. A more detailed study of the pH effect is summarized in Fig. 2, showing the variation of the net peak currents and potentials with pH of citrate buffers.

The net peak current decreases almost linearly with increasing pH (curve *1*), whereas the peak potential shifts in a negative direction with a slope of –78 mV/pH. Moreover, at a constant pH of the buffer, the peak currents enhance almost linearly with increasing the buffer concentration from 0.01

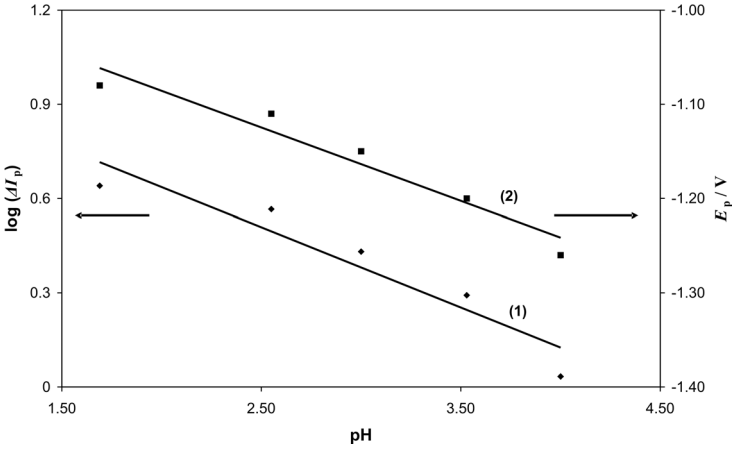

FIG. 2
Dependence of the logarithm of the net SW peak current (1, left ordinate) and net peak potential (2, right ordinate) of 1×10^{-5} M GBI on pH of citrate buffers. The other experimental conditions are the same as in Fig. 1

to 0.03 mol l^{-1}, leveling off at higher buffer concentrations (0.04–0.09 mol l^{-1}). In addition, from an analytical point of view, the pH value of 2.5 provides the highest ratio $\Delta I_p/\Delta E_{p/2}$, which is of particular importance for analytical utility of the voltammetric response.

From a mechanistic point of view, the analysis of the SW voltammetric response by altering the frequency of the potential modulation is of particular importance, as the frequency represents the typical time window of the voltammetric experiment. The dependence of the net peak current and potential for the response measured in citrate buffer at pH 2.5 is summarized in Fig. 3. The linear relationship between ΔI_p vs f is typical for various surface electrode processes, where the electroactive reactant is immobilized on the electrode surface. The linearity of the dependence E_p vs f can be improved by plotting E_p vs log f, which is characterized with a slope of –64 mV. The slope of the latter function is determined by the factor $2.303RT/(n\alpha F)$ for many irreversible electrode reaction, enabling determination of the electron transfer coefficient[25]. Nevertheless, the sort of dependencies depicted in Fig. 3, are not sufficiently selective to reveal particular electrode mechanism.

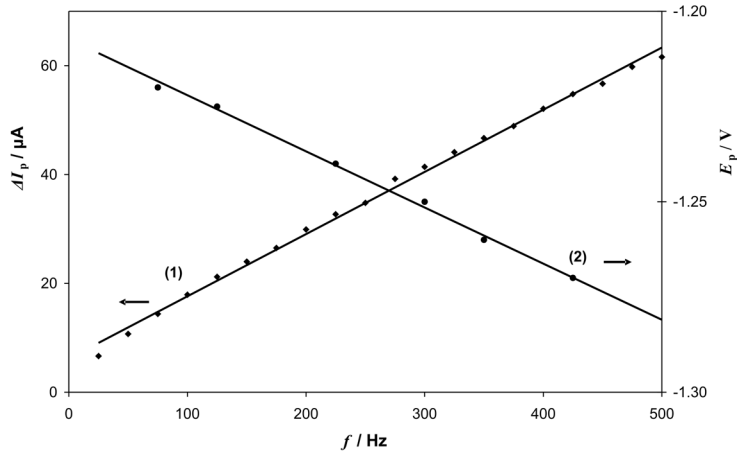

FIG. 3
Effect of the SW frequency on the net peak current (1, left ordinate) and potential (2, right ordinate) of 5×10^{-6} M GBI recorded in a citrate buffer at pH 2.5 at accumulation time 10 s and initial potential 0 V. The parameters of the potential modulation were: amplitude E_{sw} = 90 mV and step potential ΔE = 15 mV

To clarify the methodology for elucidation the electrode reaction mechanism more specifically, let us recall that the voltammetric response of any surface process can be generalized as $I = nFfA\Gamma^*\Psi$, where n is the number of electrons, F Faraday constant, A electrode surface area, Γ^* surface concentration of the electroactive reactant, f square-wave frequency and Ψ dimensionless function typical for particular electrode reaction. The product $nFfA\Gamma^*$ can be understood as an amperometric constant, whereas all intrinsic information regarding the electrode mechanism and kinetics are hidden in the properties of the dimensionless function Ψ. Apart from reversible electrode reactions, Ψ is a complex function, the properties of which depend on the kinetic parameters, mass transfer parameters as well as the frequency of the potential modulation. From the above definition of the current measured in SWV, it follows that the ratio I/f, i.e., the ratio of the real current measured at particular frequency, is proportional to the dimensionless function Ψ. Hence, in a mechanistic study, one compares the ratio I/f with the properties of the function Ψ, calculated with aid of simulations based on a theoretical model developed for the assumed electrode mechanism.

In the present system, the most likely electrode mechanisms are assumed to be (i) irreversible electrode reaction with previous adsorption of the electroactive reactant (Eqs (*1*) and (*2*)) or (ii) surface catalytic electrode mechanism based on the hydrogen evolution reaction (Eqs (*3*) and (*4*)). Both models are briefly elaborated in the Appendix.

$$\mathrm{GBI}_{(aq)} = \mathrm{GBI}_{(ads)} \qquad (1)$$

$$\mathrm{GBI}_{(ads)} + n\ \mathrm{e}^- \rightarrow \mathrm{P} \qquad (2)$$

In the first mechanism (Eqs (*1*) and (*2*)) it is assumed that GBI is the electroactive reactant, undergoing irreversible reduction to the electroinactive product P, which might be adsorbed or dissolved in the electrolyte solution (Eq. (*2*)), characterized by the surface standard rate constant k_s (s^{-1}) and electron transfer coefficient α [17,18]. Before electrochemical reduction, GBI adsorbs on the electrode surface, forming of a submonolayer, free of lateral interactions, and obeying the law of a linear adsorption isotherm associated with the adsorption constant β (cm). The justification of the mechanism (Eqs (*1*) and (*2*)) follows from the assumption that azomethine bond (C=NH), present in the guanidine moiety, can be irreversible reduced, as elaborated in refs[26–28].

In the second mechanism (Eqs (*3*) and (*4*)), GBI is electroinactive itself, rather than it undergoes adsorption and protonation reaction (Eq. (*3*)). The product of the reaction (Eq. (*3*)), $GBIH^+_{(ads)}$ is the new electroactive reactant, the reduction of which produces atomic hydrogen and regenerates back the GBI. Hence, $GBI_{(ads)}$ acts as a catalyst for the electrochemical reduction of hydrogen.

$$GBI_{(ads)} + H^+_{(aq)} = GBIH^+_{(ads)} \qquad (3)$$

$$GBIH^+_{(ads)} + e^- \rightarrow GBI_{(ads)} + H_{(ads)} \qquad (4)$$

Reactions (*3*) and (*4*) complete a hydrogen evolution surface catalytic mechanism, which was initially elaborated for the case of famotidine[19]. The protonation reaction (Eq. (*3*)) is associated with the forward, k_f' ($mol^{-1}\ l\ s^{-1}$), and backward, k_b (s^{-1}), rate constant, as well as the equilibrium constant $K' = k_f'/k_b$ ($mol^{-1}\ l$), whereas the electrode reaction (Eq. (*4*)) is characterized with the surface standard rate constant k_s and the electron transfer coefficient α. The justification for the mechanism (Eqs (*3*) and (*4*) follows from the fact that the electrochemical response of GBI occurs at potential very close to the hydrogen evolution process, having properties strongly sensitive to pH and concentration of buffers, and being detectable practically only in acidic medium[19–21,29–31].

For the mechanism (Eqs (*1*) and (*2*)), dimensionless function Ψ is primarily controlled by the adsorption parameter $\rho = 1/\beta(D/f)^{1/2}$ and the electrode kinetic parameter $\omega = k_s/f$. The adsorption parameter reflects the overall effect of adsorption, influenced by the strength of adsorption (i.e., the position of the adsorption equilibrium, β), mass transfer rate (D) and the time window of the experiment (f). The electrode kinetic parameter ω is common for all quasireversible surface processes, determining predominantly the electrochemical reversibility. Obviously, the dimensionless current function Ψ is a complex function of the frequency, as the alteration of the latter parameter affects simultaneously both parameters ρ and ω. In general, the Ψ vs f is a non-linear increasing curve, as depicted by the curves *3* and *4* in Fig. 4.

The degree of increasing of Ψ with f is proportional to the strength of adsorption. In other words Ψ increase more rapidly at stronger adsorption of the reactant, as can be concluded by comparing curves *3* and *4*, simulated for $\log \beta = 0$ (strong adsorption) and $\log \beta = -3$ (week adsorption), respec-

tively. However, the experimental curve *1* in Fig. 4, obviously mismatches the theoretically predicted behavior for the mechanism (Eqs (*1*) and (*2*)).

On the other hand, the theoretically predicted behavior for the hydrogen evolution surface catalytic mechanism is significantly different. In addition to the electrode kinetic parameter ω, Ψ is controlled by the chemical kinetic parameter $\varepsilon = (k_f + k_b)/f$ and the apparent equilibrium constant $K = k_f/k_b$. Note, that both ε and K are defined trough the new, pseudo-first order forward rate constant, $k_f = k_f' c(H^+_{(aq)})$, which is directly related to the concentration of the protons. This follows from the assumption that the concentration of protons at the electrode surface in a buffered solution is constant in the course of the voltammetric experiment[19].

The frequency of the potential modulation is expecting again to exhibit a complex effect to Ψ, through the simultaneous alteration of the two parameters ω and ε. Generally, Ψ decreases by increasing f, as illustrated by the curve *2* in Fig. 4. This is in qualitative agreement with the trend of the experimental curve *1*, depicted in the same Figure. Moreover, in the previ-

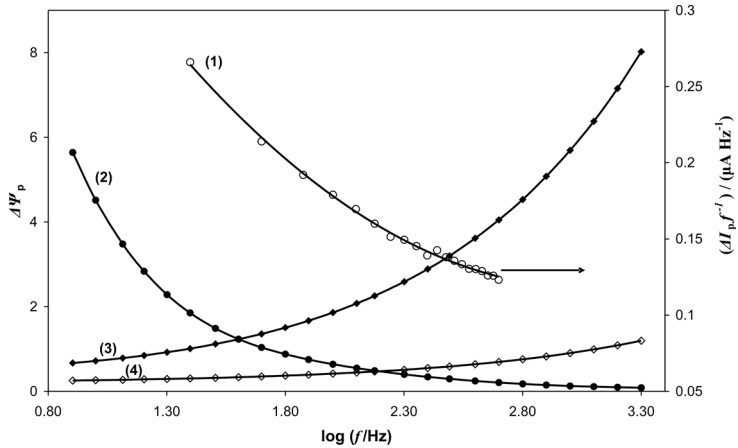

FIG. 4

Experimental results (curve 1, right axis). Logarithmic dependence of the ratio $\Delta I_p/f$ on the SW frequency, f. The conditions of the experiments were the same as in Fig. 3. *Theoretical results* (left axis). Logarithmic dependence of the dimensionless net peak current, $\Delta\Psi_p$ on the SW frequency, f for the hydrogen evolution surface catalytic mechanism (Eqs (*3*) and (*4*); curve 2) and adsorptive irreversible reductive mechanism (Eqs (*1*) and (*2*); curves 3 and 4). The conditions of the simulations were: (curve 2) pH = 1, log k_f = 3, log k_b = 0 and (curves 3 and 4) D = 5×10^{-6} cm^2 s^{-1}, log β = 0 (3) and 3 (4). The other conditions are common for both mechanisms: k_s = 1 s^{-1}, α = 0.5 and n = 1. The parameters of the potential modulation were: f = 25 Hz, E_{sw} = 50 mV and ΔE = 5 mV

ous detail analysis of the theoretical response of the mechanism (Eqs (*3*) and (*4*))[19] it has been shown that Ψ critically depends on an implicit catalytic parameter defined as $k_{cat} = k_f/f$. The log–log analysis of Ψ vs κ_{cat} is a line, which is depicted by the curve *2* in Fig. 5.

The corresponding dependence based on the experimental data is represented by the curve *1* in the same Figure, which is in well agreement with the theoretical data, implying that GBI follows the hydrogen evolution surface catalytic mechanism. This electrode mechanism also explains the linear dependence of the log I_p vs pH, shown in Fig. 2. Over the pH interval from 2 to 5, the logarithm of the net peak current of GBI decreases linearly with pH (curve *1* in Fig. 2), in accordance with the theoretically predicted dependence of log $\Delta\Psi_p$ on the log κ_{cat} (see Fig. 3 in ref.[19]). Moreover, the shift of the peak potential toward more negative values (curve *2* in Fig. 2) is a consequence of the shifting of the equilibrium (Eq. (*3*)) towards the left hand side by increasing pH. In the theoretical analysis the same effect is observed by decreasing the apparent equilibrium constant *K*.

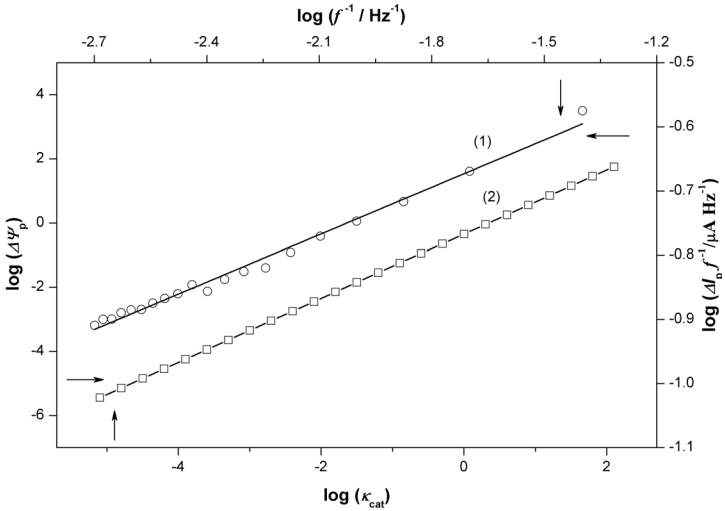

FIG. 5

Experimental results (curve 1, upper and right axis): The dependence of the logarithm of the ratio $\Delta I_p/f$ on the logarithm of the inverse frequency, f^{-1}. The experimental conditions were the same as in Fig. 3. *Theoretical results* for the hydrogen evolution surface catalytic mechanism (curve 2, left and bottom axis): The dependence of the logarithm of the dimensionless net SW peak current, $\Delta\Psi_p$ on the logarithm of the catalytic parameter κ_{cat} for the backward rate constant log $k_b = 3$. The other conditions were: $K = 1$ and log $\omega = -2.4$. The conditions of the potential modulation were the same as in Fig. 4

The hydrogen evolution surface catalytic mechanism can also provide a basis for explanation of the complex influence of the accumulation time. Assuming the adsorption of GBI molecules onto the electrode surface undergoes – as for other guanidine compounds[30] – via the guanidine group, we speculate that the decreasing of the net peak current at accumulation time longer than 50 s suggests very strong adsorption of GBI. It is accompanied by transition of the GBI protonated conformer **5** into the conformer **3**, as depicted in Scheme 2 [2]. Note that the nitrogen atoms N10 and N3 are considered to be the strongest basic sites in the GBI molecule[2,3]. The change of the protonation site from the guanidine nitrogen N10 to the imidazole nitrogen N3 hinders the catalytic effect of GBI toward hydrogen evolution reaction causing decreasing of the current at longer accumulation time.

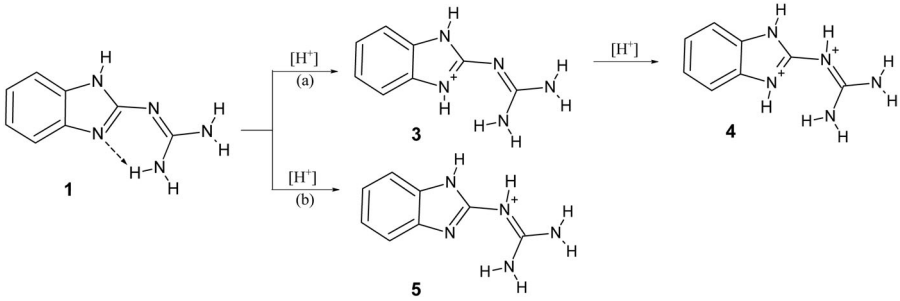

SCHEME 2
Protonation of conformer **1**: first protonation on N3 and second on N10 (a); protonation[2] on N10 (b)

Analytical Application

The SW voltammetric response of GBI at the HMDE was utilized to develop a method for quantitative determination in a citrate buffer at pH 2.5. For this purpose, all the parameters of the potential modulation such as amplitude, frequency and step potential were optimized. Their optimal values were 90 mV, 100 Hz and 15 mV, respectively. The applicability of the SWV was tested in concentration range from 1×10^{-7} to 4×10^{-6} mol l^{-1} of GBI. A linear dependence of the SW peak current on GBI concentration was obtained over the interval from 1×10^{-7} to 1×10^{-6} mol l^{-1} (Fig. 6).

The analytical characteristics of the voltammetric method are shown in Table I. Other voltammetric techniques such as linear sweep voltammetry and differential pulse voltammetry were also tested and compared, the data being summarized in Table I.

Validation of the analytical procedure for the quantitative determination was examined via evaluation of the limit of detection (LOD), limit of quantification (LOQ), repeatability, recovery and precision. Limits of detection and quantification were calculated, as $3S_b/m$ and $10S_b/m$, respectively,

TABLE I
Regression data of calibration line for quantitative determination of GBI by SWV, DPV and LSV in citrate buffer (0.1 mol l^{-1}, pH 2.5)

Parameter	SWV	DPV	LSV
Linear concentration range, μmol l^{-1}	0.1–1.0	0.4–2	0.6–3
Slope of calibration graph, A l mol^{-1}	10.8	2.14	1.22
RSD of slope	0.04	0.09	0.03
Intercept, μA	4.50	3.33	1.58
Correlation coefficient	0.997	0.992	0.996
RSD of intercept	0.035	0.06	0.05
Number of measurements	6	6	6
LOD, μmol l^{-1}	0.035	0.14	0.2
LOQ, μmol l^{-1}	0.1	0.4	0.6

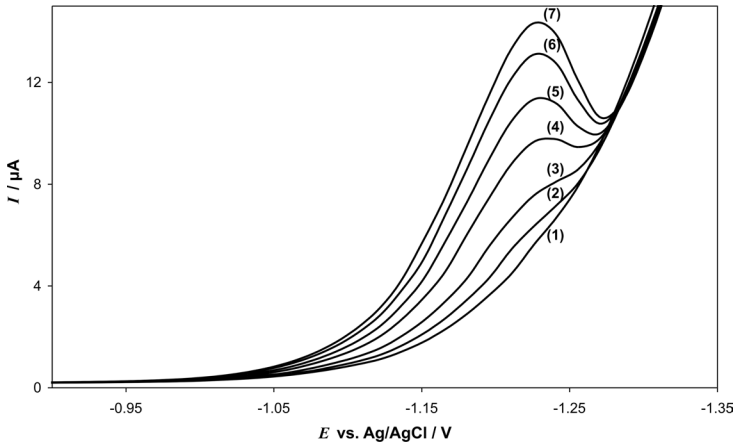

FIG. 6
SW voltammograms of GBI recorded in a citrate buffer at pH 2.5. Concentration (μmol l^{-1}) of GBI: 0 (1), 0.1 (2), 0.2 (3), 0.4 (4), 0.6 (5), 0.8 (6) and 1.0 (7). The parameters of the potential modulation were: amplitude E_{sw} = 90 mV, frequency f = 100 Hz and step potential ΔE = 15 mV. The accumulation time was 50 s and initial potential 0 V

where S_b is the standard deviation of the peak current for the blank and m slope of the calibration curve[32]. The data on the precision and recovery analysis are presented in Table II, confirming that the proposed method can be applied for quantitative determination of GBI.

The influence of cations, anions or other organic compounds (drugs) was not studied at this stage of research, as this paper is not intended to be a study of pharmacodynamic properties of GBI. We only wanted to show possibility of GBI electrochemical determination, because so far no electrochemical method of its determination was described.

TABLE II
Accuracy and precision obtained by SWV method

Added, μmol l^{-1}	Found, μmol l^{-1}	Precision RSD, %	Recovery, %[a]
0.10	0.08 ± 0.18[b]	7.6	82
0.20	0.19 ± 0.03[b]	4.5	93
0.40	0.43 ± 0.07[b]	2.5	107
0.60	0.63 ± 0.05[b]	4.0	105
0.80	0.79 ± 0.01[b]	2.5	99
1.00	0.98 ± 0.02[b]	2.3	98

[a] Recovery = 100% + [(Found – Added)/Added] × 100%. [b] $t = S/n^{1/2}$, p = 95%, n = 6.

CONCLUSION

2-Guanidinobenzimidazole is electrochemically inactive at mercury electrode, however, it adsorbs at the mercury surface and catalyzes effectively the hydrogen evolution reaction. In the case of the reaction the substrate is reproduced, the products of reaction (*4*) are transition state – analytical signal can be enhanced many times by cyclic reactions (*3*) and (*4*) at the electrode surface – so the number of electrons of catalytic reaction was not determined. The type of mechanism was evaluated under conditions of theoretical simulations and experimental results for catalytic hydrogen evolution and irreversible reduction of azomethine bond. Significant discrepancy between the studied mechanisms is depicted, and the logarithmic dependence of the ratio I/f on the SW frequency can be treated as a criterion distinguishing the character of SW voltammetric signal. It is especially useful at present when the direct current voltammetry with dropping mercury electrode are excluded from the out-of-laboratory applications. Working with SW voltammetric methods and using diluted solutions (at

the level 10^{-7}, 10^{-8} mol l^{-1}) the catalytic nature (based on hydrogen evolution) of the electrode reaction can be ascertained.

A new method for GBI determination based on hydrogen evolution catalyzed by the adsorbed compound at HMDE was developed. The important advantage of the presented studies arises from the fact that inactive at mercury electrode compound acts as electrocatalyst and can be determined by voltammetric method.

This work was supported by Grant No. 505/663 from the University of Lodz, Poland. V. M. acknowledges the support of the Ministry of Education and Science of the Republic of Macedonia with the gratitude. D. G. acknowledges the support of the CEEPUS Program in the frame of the CII-CZ-0212-04-1011 Network.

APPENDIX

Following the work of Lovriæ[17] and Osteryoung[18], the mathematical model pertinent to the electrode mechanism (Eqs (*1*) and (*2*)) can be outlined as follows.

$$\partial c_{\mathrm{GBI}}(x,t)/\partial t = D[\partial^2 c_{\mathrm{GBI}}(x,t)/\partial x^2] \qquad (A1)$$

$$t = 0,\ x \geq 0\text{: } c_{\mathrm{GBI}}(x,t) = c^*;\ \Gamma_{\mathrm{GBI}} = 0 \qquad (A2)$$

$$t > 0,\ x \to \infty\text{: } c_{\mathrm{GBI}} \to c^* \qquad (A3)$$

$$t > 0,\ x = 0\text{: } \beta(c_{\mathrm{GBI}})_{x=0} = \Gamma_{\mathrm{GBI}} \qquad (A4)$$

$$\frac{I}{nFA} = D\left(\frac{\partial c_{\mathrm{GBI}}}{\partial x}\right)_{x=0} - \frac{\mathrm{d}\Gamma_{\mathrm{GBI}}}{\mathrm{d}t} \qquad (A5)$$

$$I/nFA = k_{\mathrm{s}} \exp(-\alpha\varphi)(c_{\mathrm{GBI}})_{x=0} \qquad (A6)$$

$$\varphi = (nF/RT)(E - E^0) \qquad (A7)$$

Here, $c_{\mathrm{GBI}}(x,t)$ (mol cm^{-3}) is the concentration of dissolved GBI, which is the function of time (t) and the distance measured from the electrode surface

(x), D is the diffusion coefficient ($cm^2\ s^{-1}$), c^* is the bulk concentration, Γ_{GBI} (mol cm^{-2}) is the surface concentration of adsorbed GBI, φ is the dimensionless electrode potential relative to the standard potential, E^0, and the meaning of the other symbols have been explained in the previous sections.

Differential equation (*A1*) has been solved by applying Laplace transforms. The final numerical solution has been derived with the aid of the step-function method, which, adopted for SWV reads

$$\Psi_m = \frac{\frac{\omega \exp(-\alpha\varphi_m)}{\rho}\left[1 - \exp\left(\frac{\rho^2 m}{50}\right)\mathrm{erfc}\left(\rho\sqrt{\frac{m}{50}}\right) - \sum_{j=1}^{m-1}\Psi_j\left(\frac{2S_{m-j+1}}{\sqrt{50\pi}} + \frac{R_{m-j+1}}{\rho}\right)\right]}{1 + \frac{\omega \exp(-\alpha\varphi_m)}{\rho}\left(\frac{2}{\sqrt{50\pi}} + \frac{R_1}{\rho}\right)} . \qquad (A7)$$

Here, $\rho = 1/\beta(D/f)^{1/2}$ is the diffusion parameter, $\omega = k_s/f$ is the electrode kinetic parameter, and

$$R_m = \exp\left(\frac{\rho^2 m}{50}\right)\mathrm{erfc}\left(\rho\sqrt{\frac{m}{50}}\right) - \exp\left(\frac{\rho^2 (m-1)}{50}\right)\mathrm{erfc}\left(\rho\sqrt{\frac{m-1}{50}}\right)$$

and $S_m = \sqrt{m} - \sqrt{(m-1)}$ are numerical integration factors. For numerical integration, both time and currents have been incremented[25]. The time increment is $d = 1/(50f)$, which means that each potential pulse is divided into 25 time increments. The serial number of the time increments is designated with m.

The model for simulation of the hydrogen evolution surface catalytic mechanism is (Eqs (*3*) and (*4*)) as follows.

$$\frac{d\Gamma_{GBIH^+}}{dt} = -\frac{I}{FS} + k_f\Gamma_{GBI} - k_b\Gamma_{GBIH^+} \qquad (A8)$$

$$\frac{d\Gamma_{GBI}}{dt} = -\frac{I}{FS} + k_f\Gamma_{GBI} + k_b\Gamma_{GBIH^+} \qquad (A9)$$

$$t = 0:\ \Gamma_{GBI} = \Gamma^*_{GBI};\ \Gamma_{GBIH^+} = \Gamma^*_{GBIH^+};\ \Gamma^*_{GBI} + \Gamma^*_{GBIH^+} = \Gamma^* \qquad (A10)$$

$$t > 0: \quad \Gamma_{\mathrm{GBI}} + \Gamma_{\mathrm{GBIH^+}} = \Gamma^* \tag{A11}$$

$$\frac{I}{FS} = k_s \exp(-\alpha\varphi)\Gamma_{\mathrm{GBIH^+}} \tag{A12}$$

Here the mass transfer is neglected and only the variation of the surface concentrations is considered with time, as elaborated in ref.[19]; Γ^* is the total surface concentration, and k_f (s^{-1}) is the pseudo first-order rate constant of the forward reaction (Eq. (*3*) defined as $k_f = k_f' c(H^+_{(aq)})$. The numerical solution reads

$$\Psi_m = \frac{\omega e^{-\alpha\varphi_m} \left\{ \frac{K}{1+K}\left[e^{-\frac{m\varepsilon}{50}} + \frac{k_f}{k}\left(1 - e^{-\frac{m\varepsilon}{50}}\right)\right] + \frac{k_f}{\kappa(1+K)}\left(1 - e^{-\frac{m\varepsilon}{50}}\right) - \frac{1}{\varepsilon}\sum_{j=1}^{m-1}\Psi_j M_{m-j+1}\right\}}{1 + \frac{\omega e^{-\alpha\varphi_m}}{\varepsilon} M_1} \tag{A13}$$

Here $K = k_f/k_b$, $\varepsilon = \kappa/f$ is the chemical kinetic parameter, where $\kappa = k_f + k_b$ is the cumulative rate constant. $M_m = e^{-\{[(m-1)\varepsilon]/50\}} - e^{-[(m\varepsilon)/50]}$ is the numerical integration factor.

The recurrent formulae (*A7*) and (*A13*) have been implemented into the software package MATHCAD [33] to simulate the voltammetric response of the two electrode mechanisms.

REFERENCES

1. Castillo-Blum S. E., Barba-Behrens N.: *Coord. Chem. Rev.* **2000**, *196*, 3.
2. Hernandez-Garcia R. M., Barba-Behrens N., Salcedo R., Hojer G.: *J. Mol. Struct.* **2003**, *637*, 55.
3. Acerete C., Catalan J., Fabero F., Claramunt R. M., Sanchez-Cabezudo M., Elguero J.: *Heterocycles* **1987**, *26*, 1581.
4. Grundeman E., Graubaum H., Martin D., Schiewald E.: *Magn. Reson. Chem.* **1986**, *24*, 21.
5. Bedford G. R., Taylor P. J., Webb G. A.: *Magn. Reson. Chem.* **1995**, *33*, 389.
6. Shahrokhian S., Amini M. K., Mohammadpoor-Baltork I., Tangestaninejad S.: *Electroanalysis* **2000**, *12*, 863.
7. Garcia Calzon J., Miranda Ordieres A. J., Muniz Alvarez J. L., Lopez Fonseca J. M.: *Electroanalysis* **1996**, *8*, 326.

8. Abuin S., Centrich F., Rubies A., Companyo R., Prat M. D.: *Anal. Chim. Acta* **2008**, *617*, 184.
9. Liu Y., Zou Q. H., Xie M.-X., Han J.: *Rapid Commun. Mass Spectrom.* **2007**, *21*, 1504.
10. Salman H. M. A., Abu-Krisha M. M., El-Sheshtawy H. S.: *Can. J. Anal. Sci. Spectrosc.* **2004**, *49*, 282.
11. Jain R., Gupta V. K., Jadon N., Radhapyari K.: *Anal. Biochem.* **2010**, *407*, 79.
12. Tyszczuk K., Korolczuk M.: *Bioelectrochemistry* **2010**, *78*, 113.
13. Mirceski V., Guziejewski D., Skrzypek S., Ciesielski W.: *Croat. Chem. Acta* **2010**, *83*, 121.
14. Guziejewski D., Skrzypek S., Łuczak A., Ciesielski W.: *Collect. Czech. Chem. Commun.* **2011**, *76*, 131.
15. Guzsvany V., Papp Z., Zbiljic J., Vajdle O., Rodic M.: *Molecules* **2011**, *16*, 4451.
16. Guziejewski D., Skrzypek S., Ciesielski W.: *Food Anal. Method.* **2012**; doi:10.1007/s12161-011-9253-x.
17. Lovric M., Komorsky-Lovric S., Murray R. W.: *Electrochim. Acta* **1988**, *33*, 739.
18. O'Dea J. J., Ribes A., Osteryoung J. G.: *J. Electroanal. Chem.* **1993**, *345*, 287.
19. Mirceski V., Skrzypek S., Ciesielski W., Sokołowski A.: *J. Electroanal. Chem.* **2005**, *585*, 97.
20. Skrzypek S., Mirceski V., Ciesielski W., Sokołowski A., Zakrzewski R.: *J. Pharm. Biomed. Anal.* **2007**, *45*, 275.
21. Skrzypek S., Ciesielski W., Yilmaz S.: *Chem. Anal. (Warsaw)* **2007**, *52*, 1071.
22. Banica F. G., Ion A. in: *Encyclopedia of Analytical Chemistry* (R. A Meyers, Ed.), pp. 11115–11144. Wiley, Chichester 2000.
23. Bobrowski A., Zarębski J.: *Electroanalysis* **2000**, *12*, 1177.
24. Sequaris J. M. in: *Analytical Voltammetry* (M. R. Smyth and J. G. Vos, Eds), Vol. 27, pp. 138–140. Elsevier, Amsterdam 1992.
25. Mirceski V., Komorsky-Lovric S., Lovric M.: *Square-Wave Voltammetry: Theory and Applications*. Springer, Heidelberg 2007.
26. Kamal M. M.: *Electroanalysis* **1992**, *4*, 563.
27. Vicente F., Sanz C.: *Electrochim. Acta* **1984**, *29*, 1659.
28. Pedros F. V., Box C. S., Monge J. T.: *J. Electroanal. Chem.* **1985**, *182*, 413.
29. Banica F. G., Spataru N., Spataru T.: *Electroanalysis* **1997**, *9*, 1341.
30. Skrzypek S., Nosal-Wiercińska A., Ciesielski W.: *Collect. Czech. Chem. Commun.* **2009**, *74*, 1455.
31. Skrzypek S.: *Electroanalysis* **2010**, *22*, 2339.
32. Gumustas M., Ozkan S. A.: *Open Anal. Chem. J.* **2011**, *5*, 1.
33. *MATHCAD*. MathSoft Inc., Cambridge (MA) 1998.